HHS Public Access

Author manuscript

Environ Sci Technol. Author manuscript; available in PMC 2024 September 29.

Published in final edited form as:

Environ Sci Technol. 2022 September 06; 56(17): 12506–12516. doi:10.1021/acs.est.2c02559.

Thirdhand Exposures to Tobacco-Specific Nitrosamines through Inhalation, Dust Ingestion, Dermal Uptake, and Epidermal Chemistry

Xiaochen Tang,
Indoor Environment Group, Lawrence Berkeley National Laboratory, Berkeley, California 94720, United States

Neal Benowitz,
Clinical Pharmacology Program, Division of Cardiology, Department of Medicine, University of California San Francisco, San Francisco, California 94143, United States

Lara Gundel,
Indoor Environment Group, Lawrence Berkeley National Laboratory, Berkeley, California 94720, United States

Bo Hang,
Bioengineering & Biomedical Sciences Department, Biological Systems & Engineering Division, Lawrence Berkeley National Laboratory, Berkeley, California 94720, United States

Christopher M. Havel,
Clinical Pharmacology Program, Division of Cardiology, Department of Medicine, University of California San Francisco, San Francisco, California 94143, United States

Eunha Hoh,
School of Public Health, San Diego State University, San Diego, California 92182, United States

Peyton Jacob III,
Clinical Pharmacology Program, Division of Cardiology, Department of Medicine, University of California San Francisco, San Francisco, California 94143, United States

Jian-Hua Mao,
Bioengineering & Biomedical Sciences Department, Biological Systems & Engineering Division, Lawrence Berkeley National Laboratory, Berkeley, California 94720, United States

Manuela Martins-Green,

Corresponding Author Hugo Destaillats – Indoor Environment Group, Lawrence Berkeley National Laboratory, Berkeley, California 94720, United States; HDestaillats@lbl.gov.

Supporting Information

The Supporting Information is available free of charge at https://pubs.acs.org/doi/10.1021/acs.est.2c02559.

Experimental setup, substrates, and conditions for laboratory exposure to HONO; sweat surrogate mixture composition and TSNA formation; quantification of nicotine and TSNAs on cellulose and cotton substrate; DNA double-strand breaks caused by NNA; metabolite loss kinetics in dermally exposed mice; human dermal uptake of nicotine and NNK from tobacco-laden clothing; determination of TSNA formation rate constants in epidermal chemistry; and literature values of TSNA and nicotine concentrations in indoor air, settled dust, and indoor surfaces (PDF)

The authors declare no competing financial interest.

Department of Molecular, Cell and Systems Biology, University of California Riverside, Riverside, California 92506, United States

Georg E. Matt,
Department of Psychology, San Diego State University, San Diego, California 92182, United States

Penelope J. E. Quintana,
School of Public Health, San Diego State University, San Diego, California 92182, United States

Marion L. Russell,
Indoor Environment Group, Lawrence Berkeley National Laboratory, Berkeley, California 94720, United States

Altaf Sarker,
Bioengineering & Biomedical Sciences Department, Biological Systems & Engineering Division, Lawrence Berkeley National Laboratory, Berkeley, California 94720, United States

Suzaynn F. Schick,
Clinical Pharmacology Program, Division of Cardiology, Department of Medicine, University of California San Francisco, San Francisco, California 94143, United States

Antoine M. Snijders,
Bioengineering & Biomedical Sciences Department, Biological Systems & Engineering Division, Lawrence Berkeley National Laboratory, Berkeley, California 94720, United States

Hugo Destaillats
Indoor Environment Group, Lawrence Berkeley National Laboratory, Berkeley, California 94720, United States

ABSTRACT:

Tobacco-specific nitrosamines (TSNAs) are emitted during smoking and form indoors by nitrosation of nicotine. Two of them, *N*′-nitrosonornicotine (NNN) and 4-(methylnitrosamino)-1-(3-pyridyl)-1-butanone (NNK), are human carcinogens with No Significant Risk Levels (NSRLs) of 500 and 14 ng day^{-1}, respectively. Another TSNA, 4-(methylnitrosamino)-4-(3-pyridyl) butanal (NNA), shows genotoxic and mutagenic activity *in vitro*. Here, we present additional evidence of genotoxicity of NNA, an assessment of TSNA dermal uptake, and predicted exposure risks through different pathways. Dermal uptake was investigated by evaluating the penetration of NNK and nicotine through mice skin. Comparable mouse urine metabolite profiles suggested that both compounds were absorbed and metabolized *via* similar mechanisms. We then investigated the effects of skin constituents on the reaction of adsorbed nicotine with nitrous acid (*epidermal chemistry*). Higher TSNA concentrations were formed on cellulose and cotton substrates that were precoated with human skin oils and sweat compared to clean substrates. These results were combined with reported air, dust, and surface concentrations to assess NNK intake. Five different exposure pathways exceeded the NSRL under realistic scenarios, including inhalation, dust ingestion, direct dermal contact, gas-to-skin deposition, and epidermal nitrosation of nicotine. These results illustrate potential long-term health risks for nonsmokers in homes contaminated with thirdhand tobacco smoke.

Graphical Abstract

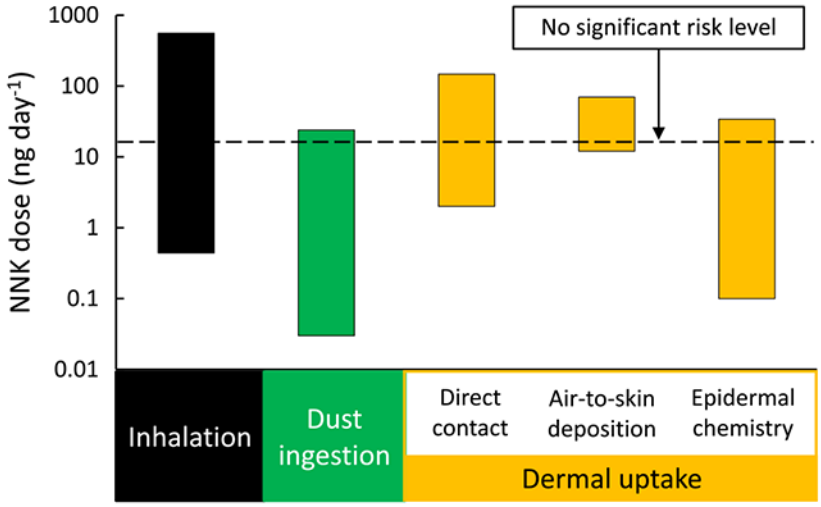

Keywords

nicotine; HONO; skin liquids; cancer risk; C57BL/6 mice

INTRODUCTION

Tobacco smoke contains hundreds of toxic chemicals, of which 72 have been identified by the International Agency for Research on Cancer (IARC) as known or possible carcinogens. Among these, 16 compounds are carcinogenic to humans (Group 1).[1] They are shown in Table S1 of the Supporting Information. Considering their physical–chemical properties, not all of these carcinogens are expected to be persistent indoors. Volatile compounds such as formaldehyde are removed effectively by ventilation after smoking has ended and do not accumulate on indoor surfaces.[2] While levels of concern of these chemicals have been reported in freshly emitted secondhand smoke (SHS), low residual air concentrations were measured up to 18 h postsmoking, which did not result in increased cancer risk[3,4] Other Group 1 carcinogens such as 1,3-butadiene and ethylene oxide are not only volatile but are also reactive, and their residence time is expected to be short (minutes to hours). By contrast, long-term exposures can be expected from semivolatile organic compounds (SVOCs) and inorganic species that can deposit on indoor surfaces and adsorb to aerosol particles and dust, thus remaining in the environment for extended time periods.

Tobacco-specific nitrosamines (TSNAs) are SVOCs of particular interest because they are unique to tobacco, and there is strong evidence of their role in the induction of cancer.[5] Their presence in freshly emitted tobacco smoke is well documented. These compounds have also been identified in the residues left behind in indoor air, dust, and surfaces after smoking, or *thirdhand smoke* (THS).[6,7] TSNAs can be produced continuously after smoking has ended as the product of nitrosation of nicotine accumulated in the indoor environment. Polycyclic aromatic hydrocarbons (PAHs) are another major group of SVOCs present in THS, from which benzo[a]pyrene is listed by IARC in Group 1. Unlike TSNAs, PAHs are emitted

by multiple combustion sources and are ubiquitous in the environment. For that reason, an association of PAH exposure with smoking is weaker than for TSNAs.[8] IARC Group 1 also includes several inorganic carcinogens such as cadmium that have been reported in fresh, secondhand, and thirdhand tobacco smoke.[9-12]

Two semivolatile TSNAs, 4-(methylnitrosamino)-1-(3-pyridyl)-1-butanone (NNK, $C_{10}H_{13}N_3O_2$) and *N*′-nitrosonornicotine (NNN, $C_9H_{11}N_3O$), have high cancer potency factors of 49 and 1.4 kg day mg^{-1}, respectively, and, in addition to their IARC Group 1 classification, are "reasonably anticipated to be human carcinogens" by the U.S. National Toxicology Program.[13] A description of their known mutagenic and carcinogenic mechanisms is provided in Section S1 (Supporting Information). Several studies linked exposure to these two compounds with human cancer in smokers.[5,14] In the State of California, the Office of Environmental Health Hazard Assessment (OEHHA) established a Prop. 65 No Significant Risk Levels (NSRLs) of 14 ng day^{-1} for NNK, and 500 ng day^{-1} for NNN.[15] The formation of these nitrosamines, as well as 4-(methylnitrosamino)-4-(3-pyridyl) butanal (NNA, $C_{10}H_{13}N_3O_2$), from the reaction of nicotine with atmospheric nitrous acid (HONO) has been reported on model indoor surfaces.[7,16] As a consequence of the large amount of nicotine present on THS-laden indoor surfaces and the constant presence of HONO (generated in combustion sources of indoor and outdoor origin and from NO_x heterogeneous chemistry),[17,18] TSNAs are expected to be produced continuously in indoor environments where tobacco smoke is present.

Integrated exposure to NNK is primarily assessed by quantifying its major metabolite (and also a carcinogen), the urine biomarker 4-(methylnitrosamino)-1-(3-pyridyl)-1-butanol, or NNAL.[8,19,20] Due to its specificity to NNK and its relatively long half-life (10 days to 3 weeks), NNAL provides a good measure of total NNK intake. However, urinary NNAL does not allow differentiating between secondhand smoke (SHS) and THS exposures in nonsmokers, nor does it provide information on the exposure route. For SHS, it is reasonable to assume that the primary pathway is inhalation. While there is no sharp transition between SHS and THS, and both exposures can coexist in smoking environments, in most cases, THS exposures become more prevalent 2–3 h after active smoking ended.[3] In conditions in which THS predominates, such as nonsmokers inhabiting a formerly-smoked-in environment, we hypothesize that dermal uptake and dust ingestion are likely to be comparable with inhalation, contributing to total exposure to TSNAs.

In this study, we provide additional insights into the mutagenicity and genotoxicity of NNA, on dermal uptake of TSNAs, and on the role of epidermal chemistry. We calculated how much TSNAs nonsmokers take in through different pathways of exposure, and compared it with established health-based guidelines. The relative contributions to total TSNA intake were estimated for inhalation, ingestion, and different dermal uptake pathways, considering realistic indoor scenarios. The inputs used in this analysis were TSNA concentrations measured in different indoor media, along with kinetic data generated in our own experiments. In addition, the correlations between TSNAs and nicotine in different media were evaluated. This information is critical to develop metrics of THS contamination that can support the implementation of effective protective measures and remediation approaches.

MATERIALS AND METHODS

Immunofluorescent DNA Damage.

Human nontumorigenic lung epithelial BEAS-2B cells were grown overnight in 4-well chamber slides (Nunc Lab-Tek). The cells were exposed to 1 μM NNA or control (DMEM media only) for 24 h and then washed three times with phosphate-buffered saline (PBS) solution. Cells were fixed and processed for immunofluorescence microscopy following an established method.[21] Incubation with rabbit anti-53BP1 antibody (A300–272A, Bethyl Laboratories) was followed by washes and incubation with secondary antibodies conjugated to Alexa Fluor 488 (Molecular Probes) and with 4′,6-diamidino-2-phenylindole (DAPI) to stain nuclear DNA. Slides were mounted in VECTASHIELD (Vector Labs), and images were captured using a Zeiss LSM 710 confocal microscope (Carl Zeiss Inc.). Images within the same data set were captured with the same exposure time so that the intensities were within the linear range and could be compared across samples.

Dermal Intake of Nicotine and NNK in Animal Model.

Nicotine and NNK were applied dermally to mice to determine the rate of elimination of these compounds when taken through chronic dermal exposure. Nicotine (50 μg per cm^2) and NKK (50 ng per cm^2) were applied once daily to the shaved backs of 2-month-old C57BL/6 mice for seven consecutive days. The nicotine and NNK doses were adjusted to reproduce their ratio in thirdhand smoke while ensuring that metabolites could be detected. Compounds were dissolved in 100% ethanol, and control animals were exposed to solvent only. Briefly, 100 μL of freshly prepared solutions (2 mg mL^{-1} nicotine and 2 μg mL^{-1} NNK) were applied daily in a 2 × 2 cm spot on the neck that does not allow for the mice to lick, to avoid possible confounding oral exposures. The daily doses were 200 μg of nicotine and 200 ng of NNK. Ethanol is a commonly used vehicle for dermal delivery, which evaporates faster than water avoiding possible runoff and enabling consistent dosage. Alternatives such as hydrocarbons, surfactants, or essential oils generally would have been more disruptive to the lipid bilayer structure in the stratum corneum.[22] Mice were fed a standard chow diet and single-housed in Tecniplast metabolic cages under similar conditions. Three animals were exposed to NNK, three were exposed to nicotine, and three were nonexposed controls. Urine was collected at the end of each day during the seven days of application, and an additional period of seven days after dermal uptake had stopped. Urine samples from different mice were not pooled and were immediately frozen at −80 °C. All animal experimental protocols were approved by the University of California, Riverside, Institutional Animal Care and Use Committee. Urine samples (300 μL) were analyzed using Liquid Chromatography with tandem mass spectrometry (LC-MS/MS) by modification of a previously described method.[23] The modification involved including the ion transition m/z 291 → 175 to simultaneously measure concentrations of 3′-hydroxycotinine (3HC) using the method developed for NNAL. The limit of quantification (LOQ) was 148 ng mL^{-1} for 3HC and 7 pg mL^{-1} for NNAL.

Simulated Epidermal Nitrosation of Nicotine.

The reaction of surface-bound nicotine with HONO in the presence of skin oils and sweat was tested in the laboratory using the experimental system described in Figure S1

(Supporting Information). HONO was generated following a method previously used in our laboratory,[7,24,25] by mixing 1 mM $NaNO_2$ (aq) and 20 mM H_2SO_4 (aq) delivered with syringe pumps at a constant rate to a continuously stirred tank, from which excess liquid was removed with a third syringe pump to maintain a steady state. Clean air was delivered to the tank at 55 mL min^{-1}, and the displaced headspace was mixed with dry air (50 mL min^{-1}) to adjust the relative humidity to 50% and the target HONO concentration to 500 ppb before the mixture was introduced into a flow exposure chamber. Individual specimens containing a known nicotine surface concentration were placed inside the flow chamber and exposed to the flow of HONO-enriched air for 1 h. The residence time of HONO (g) inside the chamber was 8.1 s. The concentration of HONO exiting the flow chamber was determined immediately prior to, during, and after each determination, by passing it through two impingers in series filled with 5 mL of 0.1 mM NaOH (aq). HONO was quantified by measuring the concentration of nitrite anions present in the impinger solutions by ion chromatography (Dionex ICS-2000). The tested specimens are described in Table S2 and illustrated in Figure S2 (Supporting Information). Specimens of cellulose and cotton were used as substrates to systematically evaluate the effect of skin oils and sweat on the nitrosation reaction. Cellulose and cotton strips (1 × 3 cm) were cut from chromatography paper and undyed clean cloth, respectively. Specimens were held in close contact with the forearm of a volunteer to transfer skin oils and sweat using a bandage that kept the materials firmly pressed against the skin during 8 h immediately prior to their use in each test. Other cellulose and cotton substrates were modified by addition of 250 μL of an artificial sweat surrogate mixture adapted from Pavilonis et al.[26] and described in Table S3 (Supporting Information). Two sets of specimens were prepared, in which the sweat surrogate mixtures had been adjusted to pH = 4 and 7, respectively, corresponding to the two extremes of the range of acidity observed in human sweat. Nicotine was added to each specimen by addition of 100 μL of a methanolic solution allowing for the solvent to evaporate, which resulted in surface concentrations of 33 μg cm^{-2}. After exposure to HONO, the specimens were extracted twice with acetic acid solution in water (0.1 mM), and extracts were split into two aliquots for the analysis of nicotine/NNN/NNK and NNA, respectively. Aliquots were alkalinized and extracted with a 40:40:15:5 pentane/dichloromethane/ethyl acetate/isopropanol mixture, preconcentrated, and analyzed by LC-MS/MS. Nicotine from the same extracts was analyzed by Gas chromatography/mass spectrometry (GC/MS). NNA was analyzed separately after being derivatized with pentafluor-ophenylhydrazine (PFPH). Additional details on the TSNA and nicotine quantification are provided in Section S2 (Supporting Information).

Predicting TSNA Daily Doses.

The following equations were used to predict the TSNA daily doses (expressed in ng day^{-1}) corresponding to different exposure pathways for a typical US adult of 80 kg body weight. The choice of concentration ranges and other inputs are described in the Results and Discussion section.

Inhalation.—The average daily dose of each TSNA (i) via inhalation (D^i_{inhal}) was determined as follows[27]

$$D^i_{\text{inhal}} = C^i_{\text{inhal}} \times V_b \times \alpha^i_{\text{inhal}} \quad (1)$$

where C^i_{inhal} is the concentration of the i-th nitrosamine in gas phase (indoor air, expressed in pg m^{-3}), $V_b = 15\,m^3\,day^{-1}$ is the daily breathing volume,[28] and α^i_{inhal} is the fraction of the compound retained during normal respiration (unitless).

Dust Ingestion.—The average daily TSNA dose corresponding to ingestion of dust (D^i_{dust}) was calculated as

$$D^i_{\text{dust}} = C^i_{\text{dust}} \times IR \times \alpha^i_{\text{dust}} \quad (2)$$

where C^i_{dust} is the concentration of the i-th nitrosamine in indoor dust (expressed in ng per gram of dust), $IR = 20\,mg\,day^{-1}$ is the indoor settled dust ingestion rate (central tendency for adults and youth >12-year old),[29] and α^i_{dust} is the bioavailability of the compound in the gastrointestinal tract (unitless).

Direct Dermal Contact.—The average daily TSNA dose from direct dermal contact with contaminated materials (D^i_{mater}) was calculated for a scenario in which an adult spends 8 h sleeping, in close contact with bedding materials contaminated with THS, as follows[30]

$$D^i_{\text{mater}} = C^i_{\text{mater}} \times S_{\text{mater}} \times \tau \times \alpha^i_{\text{mater}} \quad (3)$$

where C^i_{mater} is the surface concentration of the i-th nitrosamine on materials that are in direct contact with the skin (expressed in ng m^{-2}), $S_{\text{mater}} = 2\,m^2$ is the estimated skin surface in direct contact with THS-contaminated materials, τ is the fraction of the day spent in bed (in this scenario, $\tau = 0.33\,day^{-1}$), and α^i_{mater} is the efficiency of transfer from the material to the skin and its absorption at the epidermis (unitless).

Air-to-Skin Deposition.—In addition to direct contact with materials, air-to-skin transport is another source of dermal exposure to contaminants.[27,31-34] For this analysis, we used the model developed by Weschler and Nazaroff.[34] The daily dose for this route ($D^i_{\text{air-skin}}$) was calculated as follows

$$D^i_{\text{air-skin}} = C^i_{\text{air}} \times k^i_{\text{p\_g}} \times S_{\text{air}} \times \alpha^i_{\text{air}} \quad (4)$$

where C^i_{air} is the gas phase concentration of the i-th nitrosamine in the proximity of the body. This value may be equal to or higher than the concentration used to predict the inhalation dose (C^i_{inhal}), depending on the proximity of the skin to contaminated materials.

The parameter $k^{i}_{p\_g}$ is the indoor air transdermal permeability coefficient, S_{air} is the body surface area in contact with indoor air, and α^{i}_{air} is the deposition efficiency.

Epidermal Chemistry.—For TSNAs forming *in situ* on the skin as a byproduct of the nitrosation of adsorbed nicotine, the average daily dose (D^{i}_{chem}) was estimated as follows

$$D^{i}_{chem} = k_i \times [\mathrm{HONO}] \times C_N \times \frac{MW_{TSNA}}{MW_N} \times S_{air} \times \alpha^{i}_{chem} \quad (5)$$

where k_i is the estimated rate constant of the surface reaction of nicotine with HONO expressed in ppb^{-1} day^{-1}, [HONO] is the concentration of HONO in indoor air (in ppb), C_N is the concentration of nicotine on the skin (expressed in ng m^{-2}), MW_{TSNA}/MW_N is the molecular weight ratio between byproduct and precursor (unitless), S_{air} is the above-mentioned body surface area (in m^2), and α^{i}_{chem} is the efficiency of absorption at the epidermis (unitless).

RESULTS AND DISCUSSION

DNA Damage Caused by NNA.

Exposure of BEAS-2B human lung epithelial cells to NNA induced a significant increase in DNA strand breaks, including double-strand breaks (DSBs), the most deleterious type of DNA damage. Figure S3 (Supporting Information) illustrates DNA double-strand breaks visualized by immunofluorescence staining of P53 binding protein 1 (53BP1, green) 24 h after exposure to 1 μM NNA or control (no NNA exposure). Nuclei were visualized with DAPI staining (blue). A 3-fold increase in the number of DSBs (53BP1 foci) was observed in the NNA-exposed cells compared to the control ($p = 0.006$). These results, together with previously published experiments showing that NNA is mutagenic and genotoxic,[24,35,36] suggest that NNA can contribute to tobacco-induced cancer risk. Further evidence linking NNA with DNA damage and impaired replication and transcription in the same lung cell lines has been recently published.[37]

Nitrosamine Dermal Uptake.

Results from the mouse dermal exposure experiment are shown in Figure 1. Dermal uptake was quantified by measuring urinary levels of the nicotine and NNK metabolites 3HC and NNAL, respectively. Both 3HC and NNAL reached a steady-state concentration in urine within 24 h after the first dermal application, which was sustained during seven days of continuous dermal exposure. By contrast, in the control samples, the levels of both 3HC and NNAL were below the detection limit at all times. While nicotine levels applied to the skin were three orders of magnitude higher than NNK, the steady-state urine concentrations did not reflect that ratio. The maximum 3HC urine concentration (10 μg mL^{-1}) was less than one order of magnitude higher than that of NNAL (3.5 μg mL^{-1}). This difference could be attributed to a more effective uptake of NNK. The formation of additional nicotine metabolites (other than 3HC) was not evaluated. However, Raunio et al.[38] reported that 3HC represents 77% of the total amount of nicotine-related material in mice urine, which makes

it a good proxy for nicotine excretion. After seven daily dermal exposures, applications were discontinued, and a decrease in the concentration of both metabolites was observed at relatively similar rates. After dermal application ended on the 7th day, 3HC followed a zero-order loss kinetics, while NNAL followed first-order kinetics (Figure S4, Supporting Information). Since elimination of drugs from the body usually follows first-order kinetics, it is possible that the loss of 3HC reflected the presence of a reservoir in the skin with slow release into the circulation, as observed in a clinical case.[39] This effect could be magnified by the larger doses of nicotine applied on the skin, with respect to NNK. On the last day of measurements (day 14), urine concentrations had dropped three orders of magnitude for each of the compounds but were still excreted at significant levels in comparison to the control group. These results suggest that, in mice, the direct dermal contact of nicotine and NNK resulted in the accumulation and circulation of these chemicals and their metabolites in the body for days after exposure, potentially causing damage and alterations to the body and its organ systems.

These results are comparable to reported dermal uptake of THS components by healthy nonsmoker volunteers wearing cotton clothing that had been exposed to cigarette smoke.[40] A description of these experiments is provided in Section S3 (Supporting Information), along with a summary of nicotine and NNK biomarkers (cotinine and NNAL, respectively) detected in participants' urine (Table S4). Urinary levels of NNAL were found to increase 86-fold 8 h after exposure, whereas cotinine increased 18-fold compared to background levels.

Simulated Epidermal Nitrosation of Nicotine.

The HONO deposition onto each specimen over the 1 h exposure period (α_{HONO}, %) was determined as

$$\alpha_{HONO} = \frac{C_{up} - C_{down}}{C_{up}} \times 100 \quad (6)$$

where C_{up} is the concentration of HONO entering the flow chamber (determined as the average of the levels determined before and after each test) and C_{down} is the concentration of HONO measured downstream of the flow chamber during the exposure period, resulting from deposition and reaction on the specimen. The results corresponding to the different specimens tested are presented in Figure 2. The HONO deposition onto each specimen was measured in duplicate determinations, with very good agreement between replicates. A small fraction of HONO ($\alpha_{HONO} = 10 - 12\,\%$) was retained by clean cellulose and cotton specimens at 50% RH without the addition of nicotine. When nicotine was added to the clean substrates, the HONO deposition increased to $\alpha_{HONO} = 55 - 56\,\%$ for cellulose and 46–48% for cotton. In cellulose, the presence of added skin oils and sweat did not result in a major change in HONO deposition ($\alpha_{HONO} = 36 - 54\,\%$). However, cotton specimens that had been applied to the skin showed a dramatic drop to $\alpha_{HONO} = 1 - 5\,\%$. One possible reason for such difference with respect to cellulose is the presence of a significantly larger amount of embedded water in cotton. In cellulose and cotton specimens with added artificial sweat

at pH 4, results were comparable to the specimens applied to the skin ($\alpha_{HONO} = 43 - 46$ and 3–9%, respectively). When the sweat surrogate mixture was adjusted to pH 7, a significantly larger HONO deposition was observed on both materials ($\alpha_{HONO} = 72 - 76\,\%$ for cellulose and 35–66% for cotton), consistent with the expected larger degree of dissociation of HONO ($pK_a = 3.16$) in less acidic conditions. In summary, HONO deposition varied with the substrate, the presence of skin liquids, the water content, and surface acid–base properties.

The surface concentration of TSNAs determined in each of the tests is shown in Figure 3. There was overall good reproducibility in duplicate determinations. There was no formation of these compounds in the absence of nicotine, nor in most cases when HONO was absent (only low levels of NNN and NNA in a few specimens). While a small fraction of HONO may dismutate to form NO and NO_2, our previous work has shown negligible nitrosamine formation from the reaction of nicotine with NO or NO_2.[7] When both nicotine and HONO were present in clean substrates, the formation of NNK, NNN, and NNA was observed. The results on clean cellulose reproduce well our previously reported experiments under similar conditions, both in actual concentrations and relative levels among the three TSNAs.[7] NNA levels were highest, while NNK was present at a higher concentration than NNN. Overall concentrations were higher on cotton than on cellulose surfaces. In the presence of skin oils and sweat, several differences were observed with respect to the clean substrates. In cellulose, even if the skin liquids had not affected HONO deposition, they resulted in increased NNA concentrations by a factor ≈2 and small changes in NNK and NNN levels. In cotton, even though the HONO deposition was reduced dramatically, the yield of TSNAs increased with respect to the clean material, with NNK, NNN, and NNA all growing by a factor of ≈2. It should be kept in mind that the concentrations of nicotine and HONO were between 10^3 and 10^5 times higher than the concentrations of TSNAs formed. A reduction of one order of magnitude in HONO deposition onto cotton did not translate into a reduction in TSNA concentration. On the contrary, the apparent increased acidity of the cotton sample containing skin oils and sweat contributed to a more extensive nitrosation reaction.

The quantitative determination of nicotine, HONO, and TSNA concentrations allowed for the calculation of the reaction rates r_i corresponding to each TSNA and an estimation of the rate constant k_i for the formation of each TSNA through epidermal chemistry. The reaction rates were determined by computing the amount of each compound formed per unit surface per hour, and the rate constants were determined as follows

$$k_i = \frac{r_i}{[\mathrm{HONO}] \times C_N} \tag{7}$$

The corresponding r_i and k_i values are presented in Table S5, with more details on the calculation of k_{NNK} outlined in Section S4 (Supporting Information).

The role of skin liquids in modulating the surface chemistry was further investigated in experiments where clean substrates were modified by the addition of sweat surrogate mixtures containing a few water-soluble constituents. This approach illustrated the role of

specific inorganic (NaCl, NH_4Cl) and organic species (lactic acid, urea) and allowed for a controlled adjustment of the surface acidity. In cellulose and cotton samples to which sweat surrogate mixtures were added, practically no TSNA formation was observed except for a small amount of NNA, the most prevalent reaction product (Figure S5, Supporting Information). In most specimens in which NNA was quantified, levels were close to the LOQ When the artificial sweat was adjusted to pH 4, significant levels of NNA were observed in cellulose, but it was below LOQ in cotton. At pH 7, from the five determinations (a duplicate for cellulose and triplicate for cotton), only two were barely above the LOQ, with others not being able to be detected in both materials. The results suggest that one or several constituents of the sweat surrogate formulation inhibited the nitrosation of nicotine. In particular, lactic acid forms a strong adduct with nicotine that can interfere with the nitrosation reaction because it involves the same pyrrolidinic nitrogen atom that reacts with HONO. The formation of 1:1 nicotine adducts not only with lactic acid but also with benzoic and other carboxylic acids used as additives in the formulation of refill liquids for electronic cigarettes (often referred to as “nicotine salt”) enables increasing nicotine concentrations while avoiding harshness on the throat and upper respiratory system.[41] In our experiments, the nicotine-to-lactic acid ratio was 1:100, suggesting that, with lactic acid in a significant excess, the nitrosation of nicotine was fully inhibited. However, these concentration ratios may be far from those found in human skin. A comprehensive review of lactate in human sweat reports multiple measurements of sweat composition from different parts of the body and related to different stimuli such as exercise and heat, with lactate concentrations in the single-digit to low two digits, expressed in millimoles.[42] This is one to two orders of magnitude lower than the concentration in the sweat surrogate mixture used in the present study. In addition to lactic acid, other factors contributing to inhibiting the nitrosation could be the presence of urea in the sweat surrogate mixture and the relatively large amount of added liquid water (250 mg per specimen). In vivo spectroscopic studies have shown that the amount of moisture on the outermost layers of the epidermis (20–100 μm depth, depending on the part of the body being analyzed) is between 20 and 40% in weight.[43] Such water activity is comparable to that on cellulose and cotton specimens exposed to HONO-enriched air at 50% RH but lower than specimens that were loaded with 250 μL of aqueous sweat surrogate.

The critical role of important nonaqueous constituents, such as skin oils (or sebum), was not addressed by tests using a water-soluble surrogate mixture. Skin oils can adsorb to cotton and other textiles when worn.[44] In our experiments, skin oils were transferred to the cellulose and cotton specimens applied to the skin, as described in Figures 2 and 3. Lipids can modify the structure of the substrate and participate in HONO chemistry.[45,46] Such effects of skin oils and other constituents, which could not be observed here using aqueous sweat surrogates, warrant further investigation.

Predicted Contributions to NNK Intake from Different Exposure Pathways.

Since NNK is considered to significantly contribute to cancer risk and is more carcinogenic than NNN, we performed an analysis of the predicted contributions to total NNK intake from different routes of exposure. The predicted range of daily doses for inhalation, dust ingestion, direct dermal contact, air-to-skin deposition, and epidermal chemistry are shown

in Figure 4. The figure also includes the OEHHA NSRL value for NNK as a reference. For each exposure route, the range of doses spanned several orders of magnitude due to the variability in NNK concentrations in air, dust, and surfaces that were used as inputs to the calculation, as described in the following subsections.

Inhalation.—Table S6 (Supporting Information) summarizes reported TSNA concentrations in indoor air. In general, TSNAs in indoor air are associated with particulate matter. However, as levels of particles decrease after smoking due to ventilation removal and deposition, a persistent low level of these compounds can be found in the gas phase.[4] The range of NNK concentration in indoor air, C_{inhal}^{NNK}, was between 40 and 50,000 pg m^{-3}, reflecting different smoke aging stages and smoking prevalence. An average NNK retained fraction of $\alpha_{\text{inhal}}^{NNK} = 0.74$ was reported in determinations with smokers.[47] The predicted NNK daily intake through inhalation was between 0.44 and 560 ng day^{-1}, exceeding in many cases the NSRL. Table S6 also reports outdoor air NNK and NNN levels, which can be considered background concentrations in urban areas. Studies carried out in the US, UK, China, and Malta suggest that such background levels are in many cases below pg m^{-3} levels (parts-per-quadrillion).

Dust Ingestion.—Table S7 (Supporting Information) summarizes reported TSNA levels measured in settled indoor dust from different indoor spaces. The range of NNK concentration in settled dust, C_{dust}^{NNK}, was from 1.5 to 1190 ng g^{-1} for NNK. Studies in California included samples collected in smoker and nonsmoker homes and in a casino. Studies from Asia and Europe report significantly higher levels of TSNAs in dust from homes, government buildings, nurseries, hotel rooms, and schools compared to California. While limited in the number of samples and tested sites, these observations suggest that California results may be on the low end of a broad spectrum of values, possibly due to the successful implementation of tobacco control initiatives over the past three decades. Even considering the higher levels reported in Asia and Europe, the predicted NNK daily intake through dust ingestion for maximum bioavailability ($\alpha_{\text{dust}}^{NNK} = 1$) was between 0.03 and 24 ng day^{-1} and did not exceed the NSRL in most cases. If the analysis was based only on the California results (including those from a casino), daily NNK intake from dust ingestion would not exceed 1.7 ng day^{-1}. This analysis is based on adult dust ingestion rates, but it should be noted that exposure to children through dust ingestion may lead to a more substantial intake and risk (not included in this analysis).

Direct Dermal Uptake.—Table S8 (Supporting Information) summarizes reported TSNA levels measured on indoor surfaces of smokers' and nonsmokers' homes, along with surface concentrations determined on model materials exposed in the laboratory. To the best of our knowledge, TSNA surface concentration on human skin has not been reported. Published results on surface-bound TSNAs are fewer than those for air and dust. In these measurements, C_{mater}^{NNK} was between 3.2 and 220 ng m^{-2}. The predicted daily NNK intake through dermal transfer to the skin in direct contact with bedding materials is between 2 and 145 ng day^{-1}, assuming efficient transfer from the materials to the skin and subsequent absorption ($\alpha_{\text{mater}}^{NNK} = 1$). Under these conditions, the NNK daily dose could exceed the NSRL.

Air-to-Skin Deposition.—The Weschler/Nazaroff model used to estimate air-to-skin deposition[34] considers only compounds present in the gas phase, because particles diffuse at a slower rate than gases. The model also assumes that clothing presents negligible resistance to transport and that the flux through the skin reaches steady-state conditions. However, the effect of clothing was further investigated in a recent study, observing that clothes that were not previously contaminated with nicotine provided a degree of protection with respect to deposition from indoor air onto the skin.[48] For this analysis, we used our recently reported TSNA concentrations in the gas phase (denuder) and particle phase (filter) determined in a room-sized chamber in which samples were collected during different postsmoking times.[4] This data, along with the calculation of the gas-phase fraction (f_g) corresponding to each sample, is presented in Table S9 (Supporting Information). TSNAs were mostly particle-bound in samples collected a short time after smoking, but the opposite ($f_g \approx 1$) was observed for THS samples collected at times $t > 4$ h after smoking ended. For NNK, an indoor air transdermal permeability coefficient $k^{\mathrm{NNK}}_{p\_g} = 6.0\ \mathrm{m\ h^{-1}}$ was estimated with a model described in the Weschler/Nazaroff study[34] as a resistor in series $(1 / k_{p\_g}) = (1 / v_d) + (1 / k_{p\_b})$, where v_d is the mass-transfer coefficient for the transport of NNK from the gas phase through the skin boundary layer and k_{p_b} is the permeability coefficient through the stratum corneum/viable epidermis composite when the vehicle in contact with the skin was air. In turn, k_{p_b} was derived from the same parameter when the vehicle was water (k_{p_w}), multiplying by NNK's Henry's law constant. The value of k_{p_w} was calculated from its MW and octanol–water partitioning coefficient using an empirical relationship. For the calculation of the daily NNK doses, we used a typical adult body surface area of $S_{air} = 2\ \mathrm{m^2}$.[34] By applying a deposition efficiency $\alpha^{NNK}_{air} = 1$, the predicted values can be considered upper limit estimates as they neglect losses through desquamation and the protective effect of clothing.

For the relatively low NNK concentrations measured in chamber air at periods in which f_g was close or equal to 1 ([NNK] = 0.04–0.2 ng $\mathrm{m^{-3}}$), the predicted daily intake through air-to-skin transport was $D^{NNK}_{\text{air-skin}} = 12 - 58\ \mathrm{ng\ day^{-1}}$.

Epidermal Chemistry.—The daily amount of NNK formed on the skin through nitrosation of adsorbed nicotine by HONO was calculated for a reaction rate constant k_{NNK} between 5.5×10^{-7} and 1.6×10^{-6} $\mathrm{ppb^{-1}\ day^{-1}}$ (Table S5, Supporting Information), a typical indoor concentration of [HONO] = 50 ppb, and $S_{air} = 2\ \mathrm{m^2}$. Nicotine skin concentrations reported in Table S8 (Supporting Information) varied from $C_N = 0.3\ \mu\mathrm{g\ m^{-2}}$ in the case of children living in THS-free homes to $C_N = 157\ \mu\mathrm{g\ m^{-2}}$ for smokers' hands. Other reported values are within this range, as well as nicotine surface concentrations on silicone wristbands used as exposure samplers ($C_N = 167\ \mu\mathrm{g\ m^{-2}}$). Considering all this variability, the *in situ* formation of NNK could represent a daily dose $D^{NNK}_{\text{chem}} = 0.1 - 85\ \mathrm{ng\ day^{-1}}$, potentially exceeding the OEHHA NSRA under some conditions and representing a significant NNK exposure route. This analysis assumes that once formed, the absorption of TSNA through the epidermis is efficient ($\alpha^{NNK}_{\text{chem}} = 1$), which is consistent with the mouse dermal intake results presented above.

Implications.

One important conclusion of this study is that exposure to NNK via multiple pathways likely contributes to elevated cancer risk for adult nonsmokers exposed to THS indoors. Children are likely exposed to a greater risk, given their increased dust ingestion compared to adults, their thinner dermis, and immature organ systems. Three different dermal uptake pathways (by direct contact, air-to-skin deposition, and epidermal chemistry) are predicted to significantly contribute to total NNK intake at levels that are comparable to or even higher than inhalation. This result is in line with recent observations of higher nicotine dermal uptake *vis-a-vis* inhalation.[27] In relative terms, dust ingestion for adults seems to have a lower impact than other pathways. However, it may play a significant role for babies and toddlers, who are estimated to eat more dust than adults by being in closer proximity to the floor and mouthing objects. They are less able to metabolize, detoxify, and excrete contaminants than adults, are more easily affected at low doses, and may develop sensitization to some compounds due to early exposure, potentially leading to the development of chronic conditions.[49] While the available data set is limited, dust samples collected in California have significantly lower NNK levels with respect to studies carried out in Asian and European countries. This may be due to differences in the prevalence of smoking, weather, and building characteristics, among other factors. Further research is needed to explore these effects.

Nicotine is a widely used environmental marker of THS contamination. Comparing NNK and nicotine concentrations reported in different indoor media can provide practical correlations to predict NNK intake based on nicotine levels in studies where only nicotine is measured. The NNK/nicotine ratios from the compiled studies are plotted in Figure S6 (Supporting Information). These were derived from determinations of both compounds made in indoor air, settled dust, and indoor surfaces. One preliminary observation is that, in many cases, the NNK/nicotine ratios were in the order of 1/1000, suggesting that a quantitative correlation could be established. A similar comparison was carried out on hair that had been exposed to tobacco smoke and resulted in a similar NNK/nicotine ratio.[50] Given the large (and growing) data set available in the literature on indoor nicotine concentrations, establishing a correlation with NNK and other health-relevant THS contaminants could be of great interest to advance health risk predictions.

Considering the three studied TSNAs, NNK drives the predicted health effects based on available information. NNN is present at lower levels, and, given its lower cancer potency factor, it is reasonable to assume that its total contribution to cancer risk will be smaller than that of NNK. In the case of NNA, while its health effects are not fully assessed, a growing body of evidence suggests that it constitutes a THS contaminant of concern due to its mutagenic and genotoxic activity and because it can be formed on the skin and indoor materials at concentrations that exceeded those of NNK and NNN. More studies on the relative stability of NNA with respect to the other TSNAs are warranted. While the three TSNAs studied here are not equally carcinogenic, their combined effects may be increased from those determined for individual nitrosamines. As people are exposed to THS as a mixture, the combined effects should be considered in assessing risks associated to this preventable exposure. Tobacco control efforts should build upon knowledge of these cancer

risks in indoor environments, e.g., by promoting prompt and effective remediation to reduce contact with TSNAs.

Supplementary Material

Refer to Web version on PubMed Central for supplementary material.

ACKNOWLEDGMENTS

This study was supported by the University of California's TRDRP grants to the California Thirdhand Smoke Consortium, primarily to project 28PT-0075 (Destaillats), and also to projects 28PT-0077 (Jacob), 22RT-0121 (Martins-Green), 28PT-0079, 25IP-0023 (Quintana), 28PT-0076 (Hang), 28PT-0081, 24RT-0039 (Schick), 28PT-0078, 27IR-0019HC (Matt), and 26IR-0017 (Sarker). Laboratory resources for analytical chemistry at UCSF were supported by NIH Grant P30 DA012393 and S10 RR026437. Lawrence Berkeley National Laboratory operates under the U.S. Department of Energy contract DE-AC02–05CH11231. The authors are grateful to Kristina Bello, Lisa Lu, and Trisha Mao (UCSF) for supervising and carrying out the analysis of extracts for nicotine and TSNAs. The authors also thank Neema Adhami (UCR) for contributions to experimental work.

REFERENCES

(1). Hecht SS Research opportunities related to establishing standards for tobacco products under the family smoking prevention and tobacco control act. Nicotine Tob. Res 2012, 14, 18–28. [PubMed: 21324834]

(2). Singer BC; Hodgson AT; Nazaroff WW Gas-phase organics in environmental tobacco smoke: 2. Exposure-relevant emission factors and indirect exposures from habitual smoking. Atmos. Environ 2003, 37, 5551–5561.

(3). Sleiman M; Logue JM; Luo WT; Pankow JF; Gundel LA; Destaillats H Inhalable Constituents of Thirdhand Tobacco Smoke: Chemical Characterization and Health Impact Considerations. Environ. Sci. Technol 2014, 48, 13093–13101. [PubMed: 25317906]

(4). Tang X; Ramirez Gonzalez N; Russell ML; Maddalena RL; Gundel LA; Destaillats H Chemical changes in thirdhand smoke associated with remediation using an ozone generator. Environ. Res 2021, 198, No. 110462. [PubMed: 33217439]

(5). Hecht SS Biochemistry, biology, and carcinogenicity of tobacco specific N-nitrosamines. Chem. Res. Toxicol 1998, 11, 559–603. [PubMed: 9625726]

(6). Matt GE; Quintana PJE; Destaillats H; Gundel LA; Sleiman M; Singer BC; Jacob P; Benowitz N; Winikoff JP; Rehan V; Talbot P; Schick S; Samet J; Wang Y; Hang B; Martins-Green M; Pankow JF; Hovell MF Thirdhand tobacco smoke: Emerging evidence and arguments for a multidisciplinary research agenda. Environ. Health Perspect 2011, 119, 1218–1226. [PubMed: 21628107]

(7). Sleiman M; Gundel LA; Pankow JF; Jacob P; Singer BC; Destaillats H Formation of carcinogens indoors by surface-mediated reactions of nicotine with nitrous acid, leading to potential thirdhand smoke hazards. Proc. Natl. Acad. Sci. U.SA 2010, 107, 6576–6581.

(8). Yuan J-M; Buttler L; Stepanov I; Hecht SS Urinary tobacco smoke – Constituent biomarkers for assessing risk of lung cancer. Cancer Res. 2014, 74, 401–411. [PubMed: 24408916]

(9). Böhlandt A; Schierl R; Diemer J; Koch C; Bolte G; Kiranoglu M; Fromme H; Nowak D High concentrations of cadmium, cerium and lanthanum in indoor air due to environmental tobacco smoke. Sci. Total Environ 2012, 414, 738–741. [PubMed: 22137652]

(10). Cheng L-C; Lin C-J; Liu H-J; Li L-A Health risk of metal exposure via inhalation of cigarette sidestream smoke particulate matter. Environ. Sci. Pollut. Res 2019, 26, 10835–10845.

(11). Matt GE; Quintana PJE; Hoh E; Dodder NG; Mahabee-Gittens M; Padilla S; Markman L; Watanabe K Tobacco smoke is a likely source of lead and cadmium in settled house dust. J. Trace Elem. Med. Biol 2021, 63, No. 126656. [PubMed: 33022485]

(12). Rasmussen PE; Levesque C; Chenier M; Gardner HD; Jones-Otazo H; Petrovic S Canadian House Dust Study: Population-based concentrations, loads and loading rates of arsenic,

cadmium, chromium, copper, nickel, lead, and zinc inside urban homes. Sci. Total Environ 2013, 443, 520–529. [PubMed: 23220142]

(13). National Toxicology Program. Report on Carcinogens - Fifteenth Edition. US Department of Health and Human Services, Public Health Service. https://ntp.niehs.nih.gov/go/roc15, 2021. (accessed June 14, 2022).

(14). Hecht SS Tobacco carcinogens, their biomarkers and tobacco-induced cancer. Nat. Rev. Cancer 2003, 3, 733–744. [PubMed: 14570033]

(15). OEHHA, California Office of Environmental Health Hazard Assessment - Toxicity criteria. https://oehha.ca.gov/chemicals (accessed June 14, 2022).

(16). Sleiman M; Maddalena RL; Gundel LA; Destaillats H Rapid and sensitive gas chromatography-ion-trap tandem mass spectrometry method for the determination of tobacco-specific N-nitrosamines in secondhand smoke. J. Chromatogr. A 2009, 1216, 7899–7905. [PubMed: 19800070]

(17). Depoorter A; Kalalian C; Emmelin C; Lorentz C; George C Indoor heterogeneous photochemistry of furfural drives emissions of nitrous acid. Indoor Air 2021, 31, 682–692. [PubMed: 33020975]

(18). Lee K; Xue XP; Geyh AS; Ozkaynak H; Leaderer BP; Weschler CJ; Spengler JD Nitrous acid, nitrogen dioxide, and ozone concentrations in residential environments. Environ. Health Perspect 2002, 110, 145–149.

(19). Avila-Tang E; Al-Delaimy W; Ashley D; Benowitz N; Bernert J; Kim S; Samet J; Hecht SS Assessing secondhand smoke using biological markers. Tobacco Control 2013, 22, 164–171. [PubMed: 22940677]

(20). Matt GE; Quintana PJE; Zakarian JM; Hoh E; Hovell MF; Mahabee-Gittens M; Watanabe K; Datuin K; Vue C; Chatfield DA When smokers quit: exposure to nicotine and carcinogens persists from thirdhand smoke pollution. Tobacco Control 2017, 26, 548–556.

(21). Trego KS; Groesser T; Davalos AR; Parplys AC; Zhao W; Nelson MR; Hlaing A; Shih B; Rydberg B; Pluth JM; Tsai MS; Hoeijmakers JHJ; Sung P; Wiese C; Campisi J; Cooper PK Non-catalytic Roles for XPG with BRCA1 and BRCA2 in Homologous Recombination and Genome Stability. Mol. Cell 2016, 61, 535–546. [PubMed: 26833090]

(22). Karande P; Mitragotri S Enhancement of transdermal drug delivery via synergistic action of chemicals. Biochim. Biophys. Acta, Biomembr 2009, 1788, 2362–2373.

(23). Jacob P; Havel C; Lee DH; Yu L; Eisner MD; Benowitz N Subpicogram per milliliter determination of the tobacco-specific carcinogen metabolite 4-(methylnitrosamino)-1-(3-pyridyl)-1-butanol in human urine using liquid chromatography-tandem mass spectrometry. Anal. Chem 2008, 80, 8115–8121. [PubMed: 18841944]

(24). Hang B; Sarker AH; Havel C; Saha S; Hazra TK; Schick S; Jacob P; Rehan V; Chenna A; Sharan D; Sleiman M; Destaillats H; Gundel LA Thirdhand smoke causes DNA damage in human cells. Mutagenesis 2013, 28, 381–391. [PubMed: 23462851]

(25). Taira M; Kanda Y Continuous generation system for low-concentration gaseous nitrous acid. Anal. Chem 1990, 62, 630–633.

(26). Pavilonis BT; Weisel CP; Buckley B; Lioy P Bioaccessibility and risk of exposure to metals and SVOCs in artificial turf field fill materials and fibers. Risk Anal. 2014, 34, 44–55. [PubMed: 23758133]

(27). Beko G; Morrison GC; Weschler C; Koch HM; Palmke C; Salthammer T; Schripp T; Toftum J; Clausen G Measurements of dermal uptake of nicotine directly from air and clothing. Indoor Air 2017, 27, 427–433. [PubMed: 27555532]

(28). USEPA, U.S. Environmental Protection Agency. Exposure Factors Handbook: 2011 Edition (Final). EPA/600/R-090/052F. Chapter 6 “Inhalation Rates”. Washington, DC. https://cfpub.epa.gov/ncea/risk/recordisplay.cfm?deid=236252, 2011. (accessed on June 14, 2022).

(29). USEPA, U.S. Environmental Protection Agency. Exposure Factors Handbook, EPA/600/R-17/384F. 2017 Update for Chapter 5 “Soil and Dust Ingestion”. National Center for Environmental Assessment: Washington, DC. https://www.epa.gov/expobox/about-exposure-factors-handbook, 2017. (accessed on June 14, 2022).

(30). Boor BE; Spilak MP; Laverge J; Novoselac A; Xu Y Human exposure to indoor air pollutants in sleep microenvironments: A literature review. Build. Environ 2017, 125, 528–555.

(31). Weschler CJ; Beko G; Koch HM; Salthammer T; Schripp T; Toftum J; Clausen G Transdermal uptake of diethyl phthalate and di(n-butyl) phthalate directly from air: Experimental verification. Environ. Health Perspect 2015, 123, 928–934. [PubMed: 25850107]

(32). Weschler CJ; Nazaroff WW Semivolatile organic compounds in the indoor environment. Atmos. Environ 2008, 42, 9018–9040.

(33). Weschler CJ; Nazaroff WW SVOC exposure indoors: Fresh look at dermal pathways. Indoor Air 2012, 22, 356–377. [PubMed: 22313149]

(34). Weschler CJ; Nazaroff WW Dermal uptake of organic vapors commonly found in indoor air. Environ. Sci. Technol 2014, 48, 1230–1237. [PubMed: 24328315]

(35). Crespi CL; Penman BW; Gelboin HV; Gonzalez FJ A tobacco smoke-derived nitrosamine, 4(methylnitrosamino)-1-(3-pyridyl)-1-butanone, is activated by multiple human cytochrome P450s including the polymorphic human cytochrome P4502D6. Carcinogenesis 1991, 12, 1197–1201. [PubMed: 2070484]

(36). Jacob P; Benowitz N; Destaillats H; Gundel LA; Hang B; Martins-Green M; Matt GE; Quintana PJE; Samet J; Schick S; Talbot P; Aquilina NJ; Hovell MF; Mao J-H; Whitehead TP Thirdhand smoke: New evidence, challenges and future directions. Chem. Res. Toxicol 2017, 30, 270–294. [PubMed: 28001376]

(37). Sarker AH; Hang B Tobacco-specific nitrosamine 1-(N-methyl-nitrosamino)-1-(3-pyridinyl)-4-butanal (NNA) causes DNA damage and impaired replication/transcription in human lung cells. PLoS One 2022, 17, No. e0267839. [PubMed: 35576221]

(38). Raunio H; Pokela N; Puhakainen K; Rahnasto M; Mauriala T; Auriola S; Juvonen RO Nicotine metabolism and urinary elimination in mouse: in vitro and in vivo. Xenobiotica 2008, 38, 34–47. [PubMed: 18098062]

(39). Benowitz NL; Lake T; Keller KH; Lee BL Prolonged absorption with development of tolerance to toxic effects after cutaneous exposure to nicotine. Clin. Pharmacol. Ther 1987, 42, 119–120. [PubMed: 3595064]

(40). Schick S. Nicotine and NNK in Thirdhand Cigarette Smoke, Proceedings of the 25th Annual Meeting of the Society for Research on Nicotine and Tobacco (SRNT) Presentation SYM26A, San Francisco, CA, 2019. https://www.srnt.org/page/2019_meeting.

(41). Harvanko AM; Havel C; Jacob P; Benowitz N Characterization of nicotine salts in 23 electronic cigarette refill liquids. Nicotine Tob. Res 2020, 22, 1239–1243. [PubMed: 31821492]

(42). Derbyshire PJ; Barr H; Davis F; Higson SPJ Lactate in human sweat: a critical review of research to the present day. J. Physiol. Sci 2012, 62, 429–440. [PubMed: 22678934]

(43). Caspers PJ; Lucassen GW; Carter EA; Bruining HA; Puppels GJ In vivo confocal raman microspectroscopy of the skin: Noninvasive determination of molecular concentration profiles. J. Invest. Dermatol 2001, 116, 434–442. [PubMed: 11231318]

(44). Krifa M; Rajaganesh S; Fahy W Perspectives on textile cleaningless - detecting human sebum residues on worn clothes. Text. Res. J 2019, 89, 5226–5237.

(45). Deng H; Liu J; Wang Y; Song W; Wang X; Li X; Vione D; Gligorovski S Effect of inorganic salts on N-containing organic compounds formed by heterogeneous reaction of NO_2 with oleic acid. Environ. Sci. Technol 2021, 55, 7831–7840. [PubMed: 34086442]

(46). Liu J; Deng H; Lakey PSJ; Jiang H; Mekic M; Wang X; Shiraiwa M; Gligorovski S Unexpectedly high indoor HONO concentrations associated with photochemical NO_2 transformation on glass windows. Environ. Sci. Technol 2020, 54, 15680–15688. [PubMed: 33232600]

(47). Feng S; Plunkett SE; Lam K; Kapur S; Muhammad R; Jin Y; Zimmermann M; Mendes P; Kinser R; Roethig HJ A new method for estimating the retention of selected smoke constituents in the respiratory tract of smokers during cigarette smoking. Inhalation Toxicol. 2007, 19, 169–179.

(48). Bekö G; Morrison GC; Weschler CJ; Koch HM; Palmke C; Salthammer T; Schripp T; Eftekhari A; Toftum J; Clausen G Dermal uptake of nicotine from air and clothing: Experimental verification. Indoor Air 2018, 28, 247–257. [PubMed: 29095533]

(49). Roberts JW; Wallace LA; Camann DE; Dickey P; Gilbert SG; Lewis RG; Takaro TK Monitoring and reducing exposure of infants to pollutants in house dust. Rev. Environ. Contam. Toxicol 2009, 201, 1–39. [PubMed: 19484587]

(50). Pérez-Ortuño R; Martinez-Sanchez J; Fu M; Fernandez E; Pascual JA Evaluation of tobacco specific nitrosamines exposure by quantification of 4-(methylnitrosamino)-1-(3-pyridyl)-1-butanone (NNK) in human hair of non-smokers. Set. Rep 2016, 6, No. 25043.

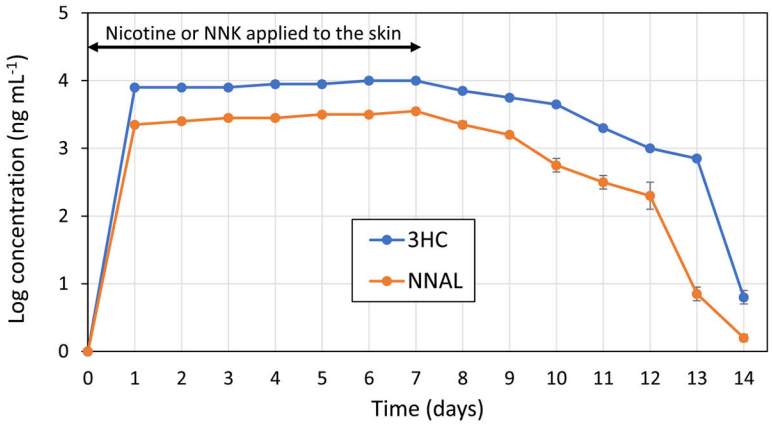

Figure 1.

Concentration of 3′-hydroxycotinine (3HC) and NNAL in urine during an initial 7-day period of continuous application of nicotine or NNK onto mice skin, followed by a 7-day clearance period. Levels of both compounds in control (nonexposed) mice were below the limit of detection. Data points represent the average from three mice and the error bars, their standard deviation.

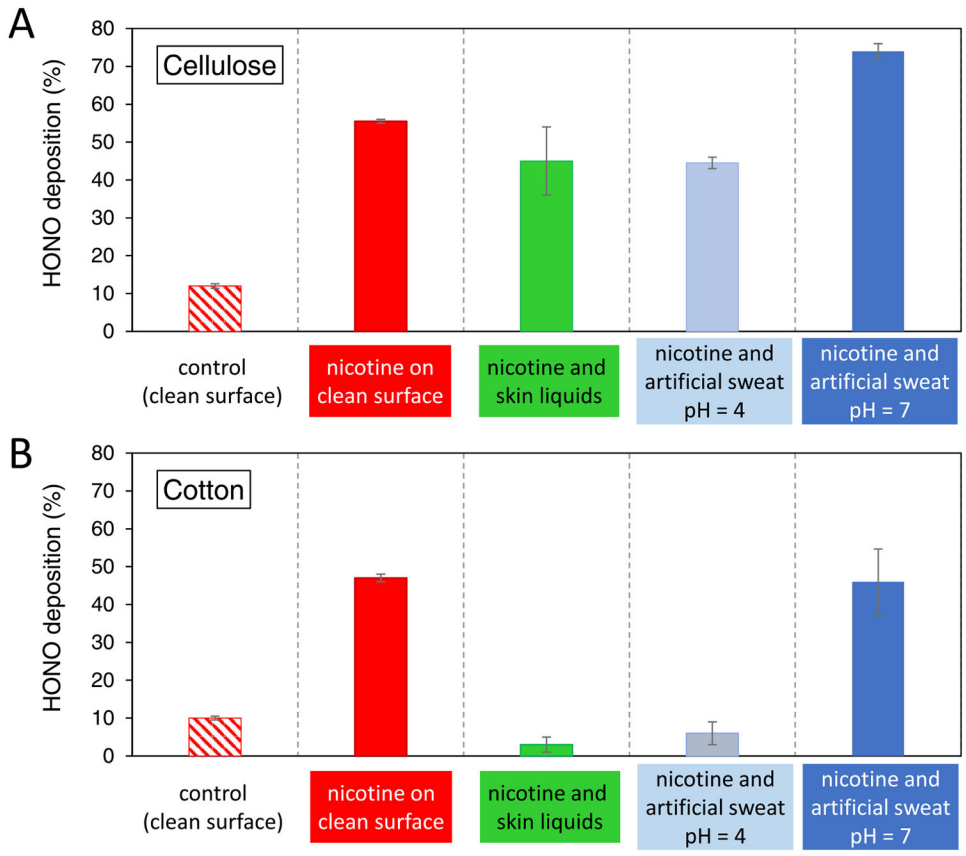

Figure 2.

HONO deposition onto different specimens of (A) cellulose and (B) cotton samples. Bars represent the average of two measurements, and the error bars show the absolute difference between determinations.

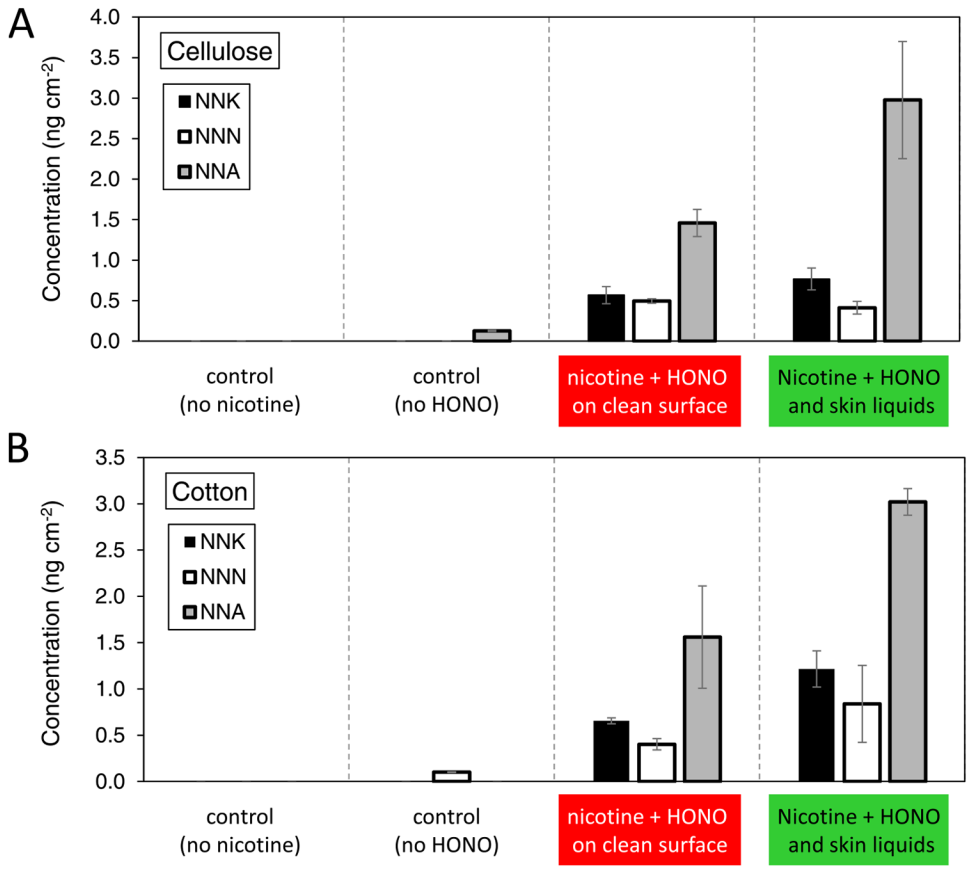

Figure 3.

TSNA surface concentration determined in experiments performed with (A) cellulose and (B) cotton specimens. Bars represent the average of two measurements, and the error bars show the absolute difference between determinations.

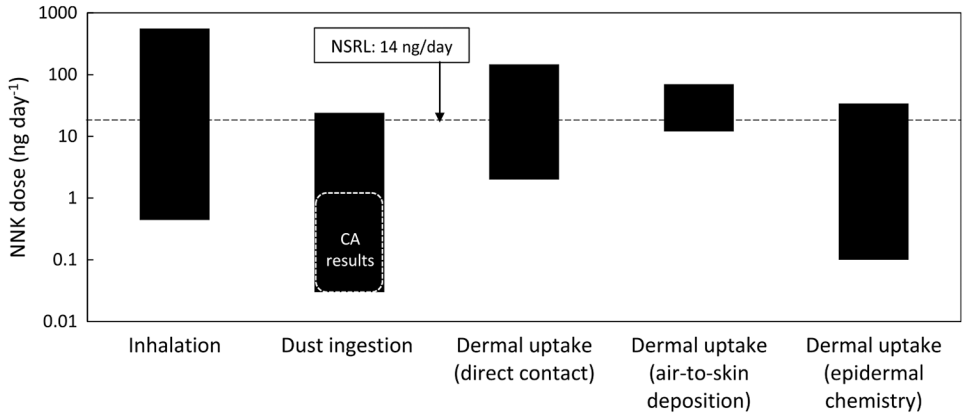

Figure 4.

Predicted daily NNK dose from typical exposures through different pathways. The bars represent the range of values to be expected based on the variability of inputs used in the calculation.